Double antinode excited quartz-enhanced photoacoustic spectrophone

Huadan Zheng, Lei Dong, Pietro Patimisco, Hongpeng Wu, Angelo Sampaolo, Xukun Yin, Shangzhi Li, Weiguang Ma, Lei Zhang, Wangbao Yin, Liantuan Xiao, Vincenzo Spagnolo, Suotang Jia, and Frank K. Tittel

Citation: Appl. Phys. Lett. **110**, 021110 (2017); doi: 10.1063/1.4973858
View online: http://dx.doi.org/10.1063/1.4973858
View Table of Contents: http://aip.scitation.org/toc/apl/110/2
Published by the American Institute of Physics

Double antinode excited quartz-enhanced photoacoustic spectrophone

Huadan Zheng,[1,2,3] Lei Dong,[1,2,a)] Pietro Patimisco,[3,4] Hongpeng Wu,[1,2,3] Angelo Sampaolo,[3,4] Xukun Yin,[1,2] Shangzhi Li,[1,2] Weiguang Ma,[1,2] Lei Zhang,[1,2] Wangbao Yin,[1,2] Liantuan Xiao,[1,2] Vincenzo Spagnolo,[3] Suotang Jia,[1,2] and Frank K. Tittel[4]
[1]*State Key Laboratory of Quantum Optics and Quantum Optics Devices, Institute of Laser Spectroscopy, Shanxi University, Taiyuan 030006, China*
[2]*Collaborative Innovation Center of Extreme Optics, Shanxi University, Taiyuan 030006, China*
[3]*Department of Electrical and Computer Engineering, Rice University, Houston, Texas 77005, USA*
[4]*Dipartimento Interateneo di Fisica, Università degli Studi di Bari and Politecnico di Bari, CNR-IFN BARI, Via Amendola 173, Bari 70126, Italy*

(Received 15 November 2016; accepted 28 December 2016; published online 10 January 2017)

A double antinode excited quartz-enhanced photoacoustic spectroscopy (DAE-QEPAS) spectrophone, employing a custom-made quartz tuning fork (QTF) and operating at the 1stt overtone resonance mode is reported. The signal phase variation along the QTF prong was investigated, and a piezoelectric transducer was introduced to compensate the phase shift between two QTF separated 1st overtone antinode points. Two sets of acoustic micro-resonators were optimized and assembled at two antinode points to improve the spectrophone performance. With the two antinodes excited by one laser source, the DAE-QEPAS spectrophone attained a sensitivity gain factor of ~100 times and ~3 times with respect to the 1st overtone resonances of a bare custom QTF and a standard on-beam QEPAS spectrophone, respectively. H_2O was selected as the target analyte and a detection limit of ~230 ppb was obtained by the DAE-QEPAS spectrophone for a 1 s integration time, corresponding to a normalized noise equivalent absorption coefficient of $1.73 \times 10^{-9}\,cm^{-1}\cdot W\cdot Hz^{-1/2}$. *Published by AIP Publishing.* [http://dx.doi.org/10.1063/1.4973858]

Quartz-enhanced photoacoustic spectroscopy (QEPAS) is a very promising technique for environmental, industrial monitoring, and medical diagnostics compared to photoacoustic spectroscopy (PAS).[1–10] The key innovation of QEPAS is to accumulate the photoacoustic energy in a small, sharply resonant quartz tuning fork (QTF), which acts as a piezoelectric acoustic transducer instead of a conventional broadband microphone. A pair of thin stainless tubes are acoustically coupled with the QTF and act as an acoustic micro-resonator (AmR) to confine the acoustic waves and enhance the QEPAS signal.[11] An assembly of two components, a QTF and an AmR, constitute a QEPAS spectrophone. The QEPAS technique combines the main characteristics of PAS with the benefits of a QTF resulting in a robust, ultra-compact, and cost-effective spectrophone.

Until 2013, QEPAS spectrophones employed only commercially available standard QTFs with a resonance frequency (f) of ~32.7 kHz in the fundamental flexural mode and a prong spacing (g) of ~300 μm.[5] Such QTFs are used in cell phones as well as watches and are optimized for timing applications. Numerous compact and sensitive trace gas sensors using QEPAS spectrophones based on standard QTFs have been designed and demonstrated.[1–3,9–11] However, the high frequency f of standard QTFs limited QEPAS applications for the detection of molecules with slow vibration-translation (V-T) relaxation rates,[12] since the V-T relaxation time τ has to be much shorter than the modulation period $1/f$. Furthermore, the small prong spacing g has prevented the use of high-power near-IR and stripe laser sources, mid-IR optical parametric oscillators (OPOs), or THz quantum cascade laser sources (QCLs) due to their limited beam profiles,[13–15] making it extremely difficult to perform laser beam focusing between the two prongs without hitting them. Therefore, several QTF designs with lower fundamental resonance frequency (a few kHz) and a larger prong spacing (>700 μm) with respect to standard QTFs have been realized, tested, and implemented in QEPAS spectrophones for gas sensing in order to overcome these limitations. This generation of QTF design was used to permit QEPAS operation with a high power fiber-amplified laser.[16] Moreover, the use of large prong spacing QTFs allowed the implementation of spectrophone configurations, such as the use of single-tube AmRs for on-beam QEPAS (SO-QEPAS) capable to obtain improved detection sensitivities.[17]

Custom QTFs with low fundamental resonance frequency also led to the implementation of QTF overtone flexural modes for QEPAS trace-gas detection.[6] An appropriate design of the QTF prong geometry can provide a higher Q factor for the 1st overtone flexural mode resonance with respect to the fundamental mode. Recently, a bare-QTF operating on its 1st overtone resonance was tested and a ~5 times higher QEPAS signal-to-noise ratio (SNR) with respect to the fundamental resonance mode was observed.[4,6] A further enhancement of the SNR (~380) was achieved by means of a SO-QEPAS spectrophone configuration.[18]

The 1st overtone flexural mode can be modeled as 2-coupled point-masses, each one positioned at an antinode and oscillating in counter-phase. The two antinodes identify the position of maximum vibration amplitudes along the prong. Hence, when a point source of sound at the 1st overtone frequency is located at the antinodes, the QEPAS signal is maximized. However, previous publications regarding the

a)Electronic mail: donglei@sxu.edu.cn

1st overtone resonance of custom QTFs focused on single antinode excitation.[4,6,18] In this letter, we report the demonstration to excite the two resonance antinode points of a custom QTF operated at the 1st overtone resonance mode simultaneously using one laser source and two dual-tubes AmRs.

The schematic diagram of the double antinode excited QEPAS (DAE-QEPAS) spectrophone is depicted in Fig. 1. A custom-made QTF with a prong length of 17 mm and prong spacing of 700 μm was employed as the acousto-electric transducer. The custom QTF was fabricated from a z-cut quartz wafer using photolithographic techniques and chromium/gold contacts were deposited on both sides of the QTF.[14] The custom QTF has a geometry with a large prong length to width ratio of 17 and is ~4.6 times larger in size with respect to a standard QTF. The fundamental and 1st overtone flexural modes resonance frequencies of the investigated custom QTF occur at ~2.8 kHz and ~17.7 kHz, respectively.[4,6] Two AmRs made of two thin stainless steel tubes were assembled in an on-beam configuration with the tubes aligned perpendicularly to the tuning fork facet (see Fig. 1(b)). The distance d between each tube and the tuning fork facet is ~20 μm (see Fig. 1(a)). The QTF is positioned between the AmRs tubes to probe the acoustic vibration excited in the gas contained inside the tubes. In a DAE-QEPAS configuration the two AmRs are positioned at heights h_1 and h_2, corresponding to the lower and higher QTF 1st overtone resonance antinode points, respectively, as shown in Fig. 1(c).

In order to determine the optimum operating conditions for the simultaneous excitation of both antinodes, the QEPAS signal amplitudes and phases of a bare QTF operated at the 1st overtone resonance were measured as a function of the sound point source position h along the QTF symmetry axis. The measurements were performed using a gas mixture

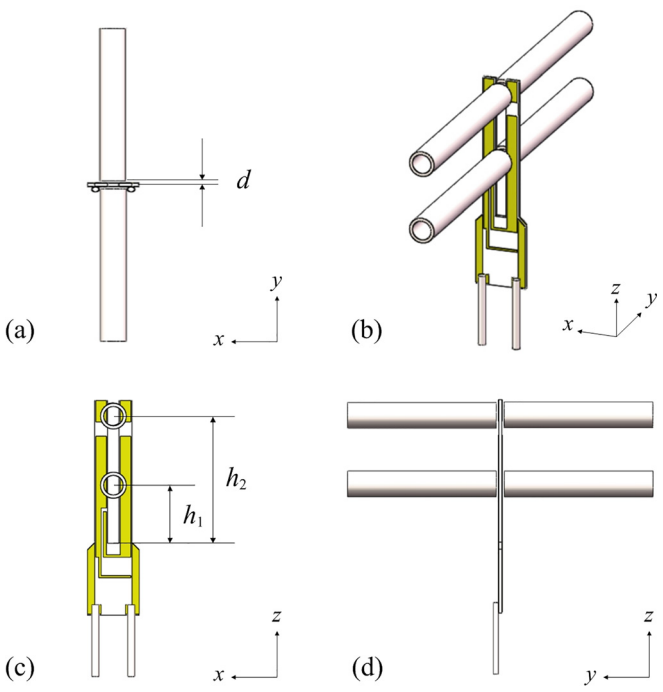

FIG. 1. Schematic diagram of the DAE-QEPAS spectrophone, (a) top view; (b) isometric view; (c) front view; and (d) side view.

composed of air and 1.8% water vapor at atmospheric pressure of 700 Torr in Taiyuan, China. The H_2O concentration was controlled by a Nafion selectively permeable membrane tubing humidifier and verified by means of direct absorption spectroscopy as described in our previous publications.[12] A pigtailed, distributed feedback (DFB) diode laser emitting at 1.37 μm was employed to generate the photoacoustic signal. The diode laser is resonant with a H_2O absorption line located at 7306.75 cm^{-1} with a line intensity of 1.8×10^{-20} cm/mol. The QEPAS signal was measured using a 2f-wavelength modulation spectroscopy (2f WMS) approach.[19–22] The laser current was sinusoidally modulated at $f/2$ by a dual-channel function generator (Tektronix AFG 3102), where f was the 1st overtone resonance frequency of the employed custom QTF. The relationship between the QEPAS signal amplitude and laser modulation depth was investigated, and an optimized modulation depth of ~0.36 cm^{-1} was used to maximize the 2f QEPAS signal. The height h of the laser spot was varied from 1 mm, close to the tuning fork base, to 17 mm corresponding to the prong tip with incremental steps of 1 mm. The piezoelectric signal generated by the QTF was pre-amplified by a custom transimpedance amplifier and then transferred to a dual-channel lock-in amplifier (Stanford SR830 DSP) to demodulate the signal in a second harmonic mode,[23–25] with a time constant of 1 s and a filter slope of 12 dB/Oct. A personal computer (PC) equipped with a data acquisition (DAQ) card was used to record and analyze the experimental data.

The 2f-QEPAS in-phase and quadrature signal amplitudes depicted in Fig. 2(a) show a minimum at $h = 12$ mm and two local maxima located at $h = 8$ mm and $h = 16$ mm, near the positions of the two antinode points. The decrease for $h > 16$ mm is caused by sound waves leaking from the QTF opening. The phase of the 2f-QEPAS overtone signal (see Fig. 2(b)) decreases from $h = 1$ mm to $h = 17$ mm and the slope of the curve shows a sharp shift at $h = 12$ mm. The nodal point at $h = \sim 13$ mm indicates that the vibrational phase inverts its sign.[6] The phase shift between the two antinode points is $\Delta \sim 180°$. The prong lateral displacement D of the QTF 1st overtone resonance as a function of h was given by

$$D = A\left\{\cosh(kh) - \cos(kh) + \frac{\sin(kL) - \sinh(kL)}{\cos(kh) + \cosh(kh)}[\sinh(kh) - \sin(kh)]\right\}, \quad (1)$$

where A was the resonance amplitude, L was the QTF prong length, and kL was 4.694, respectively.[4] The lateral displacement of the two antinodes reached the maximum at $h = 8$ mm (positive) and 17 mm (negative), which coincided with the 180° phase shift in this experiment. Therefore, the phase difference has to be compensated to excite the two antinodes simultaneously and maximize the QEPAS signal using the same laser source.

The diameter and length of the two tubes that compose the AmRs have a significant impact on the QEPAS spectrophone performance and therefore must be optimized as well.[2,11,23] Three types of stainless tubes with different outer diameters (ODs) and inner diameters (IDs) were evaluated in

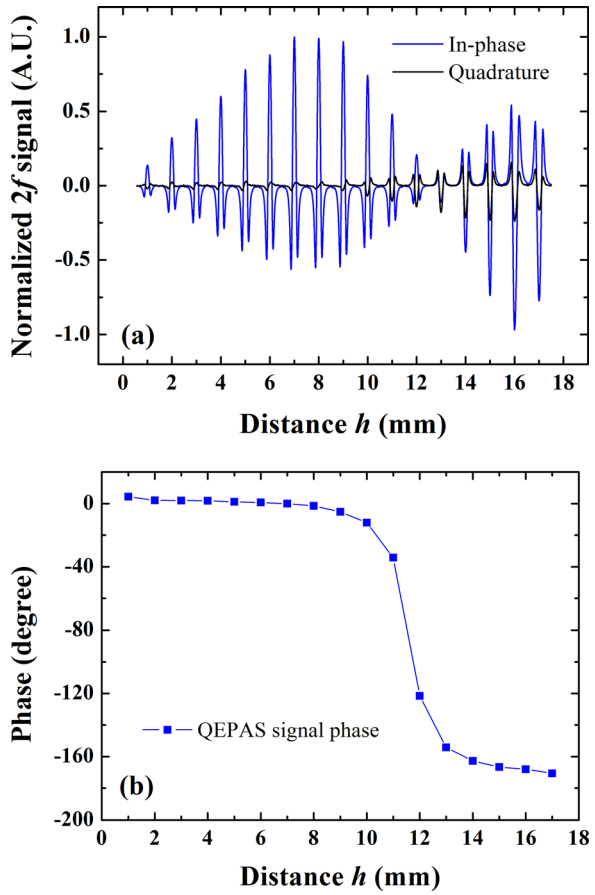

FIG. 2. 2*f* QEPAS in-phase and quadrature signals (panel (a)) and related phase difference (panel (b)) measured for the bare custom QTF as a function of *h*.

the QEPAS on-beam configuration. The parameters of the investigated QEPAS spectrophones are shown in Table I. The length of each single tube was set to 9.5 mm, which corresponds to half of the acoustic wavelength λ for the QTF 1st overtone resonance frequency *f* of ~17.7 kHz. The two AmR tubes were located at $h = 8$ mm (corresponding to the position of the lower antinode). The 1st overtone resonance frequencies of the three QEPAS spectrophones were nearly the same, while the AmR #2 with an ID of 1.3 mm showed the lowest *Q* factor of 11 680 and a maximum equivalent resistance of 172.09 kΩ, indicating that the QEPAS spectrophone based on AmR #2 provides the highest acoustic coupling efficiency.[26] Therefore, we selected AmR #2 and then proceeded to optimize its length.

The tube lengths were varied from 9.5 mm (~$\lambda/2$) to 5 mm (~$\lambda/4$). The largest QEPAS SNR was measured for AmR #2 with each tube length of 8.5 mm, providing a ~31 times higher SNR than that obtained using a bare custom QTF. Based on this analysis, two AmR#2 (ID = 1.3 mm and l = 8.5 mm) were assembled in an on-beam configuration and positioned at $h_1 = 8$ mm and $h_2 = 16$ mm, respectively. With respect to the 1st overtone resonance of the bare custom QTF falling at $f_1 = 17\,741.41$ Hz with a *Q* factor = 12 770, the corresponding DAE-QEPAS 1st overtone resonance shifts by <1 Hz to 17 742.13 Hz and the *Q* factor reduces to 7790, which means a higher QEPAS acoustic coupling efficiency.[2]

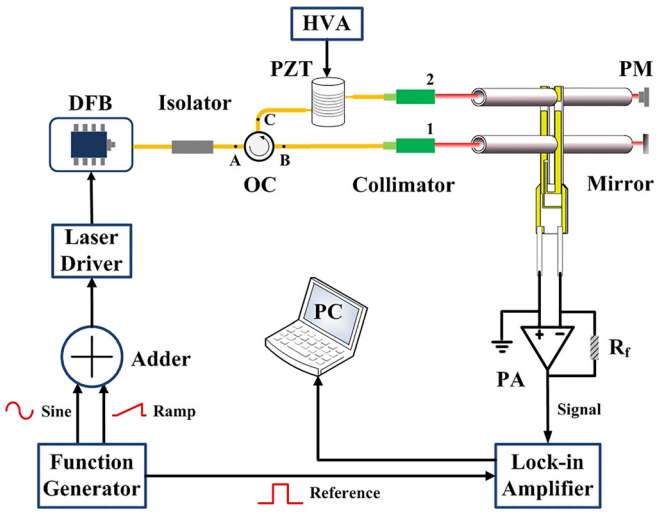

FIG. 3. Schematic of the DAE-QEPAS apparatus. DFB: distributed feedback diode laser; OC: optical circulator; PZT: piezoelectric transducer; HVA: high voltage amplifier; PM: power meter; PA: pre-amplifier; and PC: personal computer.

The schematic of the DAE-QEPAS setup is depicted in Fig. 3. The fiber pigtail of the diode laser was connected to an optical isolator with an isolation of 58 dB to prevent unwanted feedback. The laser beam passed from the optical circulator (OC) port A to port B and was then aligned by a fiber-coupled collimator (OZ optics, Ltd., Model LPC-01) to pass through the lower AmR.[27] The collimated beam diameter was ~200 μm with a divergence angle of <9 mrad with respect to a plane perpendicular to the QTF. An aluminum mirror (Daheng Optics) was placed behind the lower AmR to reflect the laser beam back through the OC from port B to port C. With the removal of the fiber cladding, the bare single mode fiber (SMF) was coiled around a piezoelectric transducer (PZT), and a custom-made high voltage amplifier (HVA) was used to drive the PZT deformation to change the optical path difference in the fiber serving as a phase compensator.[27] The laser beam exiting from the OC port C was aligned by a fiber-coupled collimator to pass through the higher AmR. A power meter was positioned after the higher

TABLE I. QEPAS spectrophone parameters based on three AmRs with different diameters. l: AmR tube length, OD: AmR tube outer diameter, and ID: AmR tube inner diameter.

	AmR tube geometrical parameters			Spectrophone electrical parameters		
	l (mm)	OD (mm)	ID (mm)	*f* (Hz)	*Q* factor	Resistance (kΩ)
AmR #1	9.5	1.38	1.2	17741.69	12090	166.53
AmR #2	9.5	1.58	1.3	17741.67	11679	172.09
AmR #3	9.5	2.13	1.65	17741.63	12240	164.51

AmR to monitor the laser power and for optical alignment. A 10 mHz slow voltage ramp signal was generated by the function generator and fed to the diode laser to scan its wavelength across the selected H_2O absorption line.

The PZT phase compensator was used to adjust the phase between the two laser beams passing through the two AmRs in order to maximize the QEPAS signal. The laser beam passed twice through the lower AmR and once through the higher AmR, exciting the two QTF resonance antinodes simultaneously with the phase compensated. The optical power exiting from the lower collimator was measured to be 13 mW. Mirror reflection and coupling losses into the lower collimator, the OC insertion loss, and a coupling loss in the SMF reduced the laser output power from the higher collimator to 8 mW.

Figure 4 depicts the QEPAS spectra obtained for a gas mixture composed of 1.8% H_2O in standard air at 700 Torr and employing: (i) the DAE-QEPAS configuration; (ii) the standard on-beam QEPAS configuration with an AmR positioned at $h = 8$ mm; and (iii) the bare QTF. All three configurations operated at the 1st overtone resonance mode. In the DAE-QEPAS configuration, we first enabled the laser beam from OC port B, i.e., only the lower antinode was excited. The signal amplitude of 140 mV provided by the double pass of the laser beam through the QTF at h_1 is more than twice the signal amplitude recorded for the standard on-beam configuration of 56.5 mV. Subsequently, the laser beam from OC port C was enabled in order to excite both antinodes. The DAE-QEPAS signal was maximized by adjusting the laser phase by means of the PZT compensator and a maximum signal amplitude of 172.2 mV was obtained, which is ~3 times higher than that obtained with the standard on-beam QEPAS and ~100 times higher than that obtained with the bare QTF (see Fig. 4). The 1σ-noise of the DAE-QEPAS spectrophone was 2.1 μV, measured with the laser wavelength tuned away from the H_2O absorption line and is comparable with a 1σ-noise level of 1.6 μV obtained with the bare QTF. The measured DAE-QEPAS SNR was 82 000, leading to a 1σ detection limit of 230 ppb for H_2O detection for a 1 s integration time. This corresponds to a normalized noise equivalent absorption (NNEA) of 1.73×10^{-9} cm^{-1}·W·Hz$^{-1/2}$ for a laser power of 13 mW.

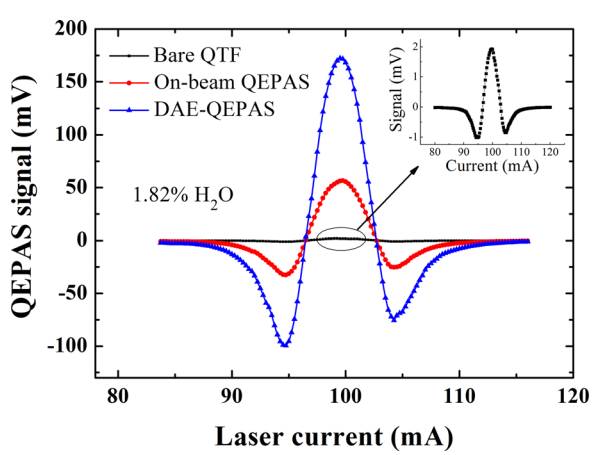

FIG. 4. Comparison between the QEPAS spectra measured using a bare custom QTF, a standard on-beam QEPAS spectrophone, and DAE-QEPAS spectrophone configurations operating at the QTF 1st overtone resonance mode. Inset: expanded view of the QEPAS spectrum measured with a bare QTF.

In conclusion, we demonstrated the realization of a DAE-QEPAS spectrophone using a custom-made QTF operating at the 1st overtone flexural mode resonance. A sensitivity gain factor of ~100 times and ~3 times was achieved with respect to a bare custom QTF and a standard on-beam QEPAS spectrophone, respectively. Such a high sensitivity gain factor is the result of the simultaneous excitation of two antinodes by means of a three-fold passage of the laser beam through two different sets of AmRs. The DAE-QEPAS spectrophone employing one laser source to excite two antinodes points makes the best possible use of the laser power without involving resonant cavity enhancement techniques, such as I-QEPAS.[28] The DAE-QEPAS configuration minimizes the sensor power consumption and cost. In addition, the phase difference between the two resonance antinodes opens approaches for optical balanced detection. The DAE-QEPAS spectrophone can also be used with free-space lasers, benefitting from the large prong spacing of the custom QTF. However, an optical phase shifter must be used to compensate the phase shift between the low and high antinodes. Further improvement of the detection sensitivity can either be achieved by assembling two single-tube AmRs exploiting the SO-QEPAS configuration or by designing and implementing an octupole gold pattern configuration in order to increase the charge collection efficiency of the 1st overtone flexural mode resonance.

Lei Dong acknowledges the support from National Natural Science Foundation of China (Grant Nos. 61622503, 61575113, and 61275213). Huadan Zheng acknowledges the support from Shanxi Scholarship Council of China (Grant No. 0011). Frank Tittel acknowledges the support from the National Science Foundation (NSF) ERC MIRTHE award and the Robert Welch Foundation (Grant C-0586). The authors from Dipartimento Interateneo di Fisica di Bari acknowledge the financial support from two Italian research projects: PON02 00675 and PON02 00576.

[1]A. A. Kosterev, Y. A. Bakhirkin, R. F. Curl, and F. K. Tittel, Opt. Lett. **27**, 1902 (2002).
[2]L. Dong, H. Wu, H. Zheng, Y. Liu, X. Liu, W. Jiang, L. Zhang, W. Ma, W. Ren, W. Yin, S. Jia, and F. K. Tittel, Opt. Lett. **39**, 2479 (2014).
[3]K. Liu, X. Guo, H. Yi, W. Chen, W. Zhang, and X. Gao, Opt. Lett. **34**, 1594 (2009).
[4]F. K. Tittel, A. Sampaolo, P. Patimisco, L. Dong, A. Geras, T. Starecki, and V. Spagnolo, Opt. Express **24**, A682 (2016).
[5]P. Patimisco, G. Scamarcio, F. K. Tittel, and V. Spagnolo, Sensors **14**, 6165 (2014).
[6]A. Sampaolo, P. Patimisco, L. Dong, A. Geras, G. Scamarcio, T. Starecki, F. K. Tittel, and V. Spagnolo, Appl. Phys. Lett. **107**, 231102 (2015).
[7]H. Yi, R. Maamary, X. Gao, M. W. Sigrist, E. Fertein, and W. Chen, Appl. Phys. Lett. **106**, 101109 (2015).
[8]Z. Li, C. Shi, and W. Ren, Opt. Lett. **41**, 4095 (2016).
[9]Y. Ma, X. Yu, G. Yu, X. Li, J. Zhang, D. Chen, R. Sun, and F. K. Tittel, Appl. Phys. Lett. **107**, 021106 (2015).
[10]T. N. Ba, M. Triki, G. Desbrosses, and A. Vicet, Rev. Sci. Instrum. **86**, 023111 (2015).
[11]L. Dong, A. A. Kosterev, D. Thomazy, and F. K. Tittel, Appl. Phys. B **100**, 627 (2010).
[12]X. Yin, L. Dong, H. Zheng, X. Liu, H. Wu, Y. Yang, W. Ma, L. Zhang, W. Yin, L. Xiao, and S. Jia, Sensors **16**, 162 (2016).
[13]J. P. Waclawek, R. Lewicki, H. Moser, M. Brandstetter, F. K. Tittel, and B. Lendl, Appl. Phys. B **117**, 113 (2014).

[14]S. Borri, P. Patimisco, A. Sampaolo, H. E. Beere, D. A. Ritchie, M. S. Vitiello, G. Scamarcio, and V. Spagnolo, Appl. Phys. Lett. **103**, 021105 (2013).
[15]M. Lassen, L. Lamard, Y. Feng, A. Peremans, and J. C. Petersen, Opt. Lett. **41**, 4118 (2016).
[16]H. Wu, A. Sampaolo, L. Dong, P. Patimisco, X. Liu, H. Zheng, X. Yin, W. Ma, L. Zhang, W. Yin, V. Spagnolo, S. Jia, and F. K. Tittel, Appl. Phys. Lett. **107**, 111104 (2015).
[17]H. Zheng, L. Dong, A. Sampaolo, H. Wu, P. Patimisco, X. Yin, W. Ma, L. Zhang, W. Yin, V. Spagnolo, S. Jia, and F. K. Tittel, Opt. Lett. **41**, 978 (2016).
[18]H. Zheng, L. Dong, A. Sampaolo, P. Patimisco, W. Ma, L. Zhang, W. Yin, L. Xiao, V. Spagnolo, S. Jia, and F. K. Tittel, Appl. Phys. Lett. **109**, 111103 (2016).
[19]L. Dong, J. Wright, B. Peters, B. A. Ferguson, F. K. Tittel, and S. McWhorter, Appl. Phys. B **107**, 459 (2012).
[20]M. Köhring, S. Böttger, U. Willer, and W. Schade, Opt. Express **21**, 20911 (2013).
[21]F. Wang, J. Chang, Q. Wang, Y. Liu, Z. Liu, Z. Qin, and C. Zhu, Opt. Commun. **381**, 152 (2016).
[22]J. P. Waclawek, H. Moser, and B. Lendl, Opt. Express **24**, 6559 (2016).
[23]H. Wu, L. Dong, W. Ren, W. Yin, W. Ma, L. Zhang, S. Jia, and F. K. Tittel, Sens. Actuators, B **206**, 364 (2015).
[24]Y. Cao, N. P. Sanchez, W. Jiang, R. J. Griffin, F. Xie, L. C. Hughes, C. Zah, and F. K. Tittel, Opt. Express **23**, 2121 (2015).
[25]L. Dong, V. Spagnolo, R. Lewicki, and F. K. Tittel, Opt. Express **19**, 24037 (2011).
[26]Y. Liu, J. Chang, J. Lian, Z. Liu, Q. Wang, and Z. Qin, Sensors **16**, 214 (2016).
[27]X. Liu, H. Wu, Y. Liu, L. Dong, W. Ma, L. Zhang, W. Yin, and S. Jia, in *Proceedings of the Pro Optics for Solar Energy* (OSA, 2015), p. JTu5A-36.
[28]P. Patimisco, S. Borri, I. Galli, D. Mazzotti, G. Giusfredi, N. Akikusa, M. Yamanishi, G. Scamarcio, P. De Natale, and V. Spagnolo, Analyst **140**, 736 (2015).